

Binding energy referencing in X-ray photoelectron spectroscopy: expanded data set confirms that adventitious carbon aligns to the vacuum level

Grzegorz Greczynski

*Thin Film Physics Division, Department of Physics (IFM), Linköping University,
SE-581 83 Linköping, Sweden*

Abstract

The correct referencing of the binding energy (BE) scale is essential for the accuracy of chemical analysis by *x*-ray photoelectron spectroscopy. The C 1s C-C/C-H peak from adventitious carbon (AdC), most commonly used for that purpose, was previously shown to shift by several eVs following changes in the sample work function ϕ_{SA} , thus indicating that AdC aligns to the sample vacuum level (VL). Here, results from a much larger sample set are presented including 360 specimens of thin-film samples comprising metals, nitrides, carbides, borides, oxides, carbonitrides, and oxynitrides. Irrespective of the material system the C 1s peak of AdC is found to follow changes in ϕ_{SA} fully confirming previous results. Several observations exclude differential charging as plausible explanation. All experimental evidence points instead to the VL alignment at the AdC/sample interface as the source of shifts. Should the C 1s peak of AdC be used for spectra referencing the measurement of sample work function is necessary, irrespective of whether samples are measured grounded or insulated from the spectrometer.

Reliable binding energy referencing is crucial in XPS as it ensures that peaks appear at correct values so that by comparing to literature or data bases assignments to chemical states can be made. To be able to make reliable chemical bonding assessments, the instruments' energy scale needs to be correctly calibrated,^{1,2} and a reliable energy reference from the sample of interest must be available. The former procedure, performed on a regular basis, ensures that the instrument works correctly, i.e., that the peaks from standard samples (typically sputter-etched metals such as Au, Ag, and Cu) appear at the correct positions on the binding energy scale.^{1,3} This, however, does not guarantee that the same holds for signals from any other sample outside the calibration set. The reason is the occurrence of sample charging, which, with the exception for metals making good contact to the spectrometer, is an unknown quantity. For that reason, the reference signal from the sample itself is required if extracted E_B values should have an absolute character.

By far the most common way to charge reference XPS spectra is to use the E_B of the C-C/C-H component of the C 1s spectrum from adventitious carbon (AdC) layer present on majority of samples.⁴ C 1s peak is then set at the arbitrary chosen value from the range 284.6-285.0 eV.^{5,6} The method was most frequently criticized in 70's and 80's for the unknown nature of AdC, uncertain electrical equilibrium with the surface it accumulates on, and the C 1s E_B varying with the AdC thickness.^{7,8,9,10,11,12,13,14,15} Despite that none of the objections were disproved, the method has gained tremendously in popularity since then, predominantly due to its simplicity. More structured criticism came during recent years from our lab, based on the systematic studies of thin film samples deposited on conducting substrates covering different materials systems.¹⁶ We reported that the AdC signature depends on the substrate type, exposure time, and the environment,^{17,18} which confirms the earlier doubts.

In the follow up paper,¹⁹ we analyzed the BE of the C 1s peak from nearly a hundred AdC layers accumulating on a whole range of substrates including metals, nitrides, carbides,

oxides, borides. The E_B^F of the C-C/C-H peak was found to vary over an alarmingly large range, from 284.08 to 286.74 eV, depending on the substrate, clearly disproving the common assumptions. Irrespectively of the materials system studied, the C 1s E_B^F correlated to the sample work function ϕ_{SA} , such that the sum $E_B^F + \phi_{SA}$, corresponding to the binding energy referenced to the vacuum level E_B^V , was nearly constant at 289.58 ± 0.14 eV. The latter indicates that AdC aligns to the sample vacuum-level (VL),¹⁹ which, as established in the early days of XPS,^{20,21,22} implies that a complementary measurement of ϕ_{SA} has to be performed if the C 1s peak of AdC should serve the purpose of binding-energy scale referencing. The C 1s BE should then be set at $289.58 - \phi_{SA}$ eV, and all other core levels should be aligned accordingly.¹⁹

Here, previous finding of the VL alignment at the AdC/sample interface is tested for a much broader sample set comprising 360 thin-film specimens spanning a wide range of material systems such as metals, nitrides, carbides, borides, oxides, carbonitrides, and oxynitrides. The list of samples is included in the supplementary file. The samples are grown by magnetron sputtering methods from elemental as well as compound targets, operated either in Ar or in (Ar/N₂) gas mixture. Substrates include Si(001), Al₂O₃(111), and steel. Experiments are performed in various vacuum systems with widely varying background pressures that range from ultra-high vacuum (UHV) to high-vacuum conditions. The growth temperature T_s is from RT (23 °C) to 900 °C, while the venting temperature T_v (temperature at which samples are first exposed to the ambient)²³ ranges from RT to 330 °C. Film thicknesses determined from cross-sectional scanning electron microscopy analyses range from 2 to 2830 nm. Samples have been exposed to the ambient environment for time periods ranging from several weeks to a few years.

All analyzes are performed in the same spectrometer (Axis Ultra DLD from Kratos Analytical) employing monochromatic Al K α radiation source ($h\nu = 1486.70$ eV). The base pressure during analyses is better than 1.1×10^{-9} Torr (1.5×10^{-7} Pa). Immediately after XPS analyses the sample work function measurements are conducted by ultraviolet photoelectron

spectroscopy (UPS) with unmonochromatized He I radiation ($h\nu = 21.22$ eV) and negatively biased samples. ϕ_{SA} is assessed from the secondary-electron cutoff energy in the He I UPS spectra by a linear extrapolation of the low-kinetic-energy electron tail towards the BE axis,^{24,25} with a precision of ± 0.05 eV. ϕ_{SA} obtained from the sputter-cleaned reference Au sample is 5.13 eV, in very good agreement with the textbook values that range from 5.0 to 5.4 eV.²⁴ The calibration of the binding-energy scale is confirmed by examining sputter-cleaned Au, Ag, and Cu samples.^{1,3} The charge neutralizer was not used in any of the reported experiments. For all samples that exhibit the Fermi level cut-off XPS valence band (VB) spectra are acquired to confirm whether the FE is at 0 eV on the BE scale, thus proving that the samples are in good electrical contact to the spectrometer.

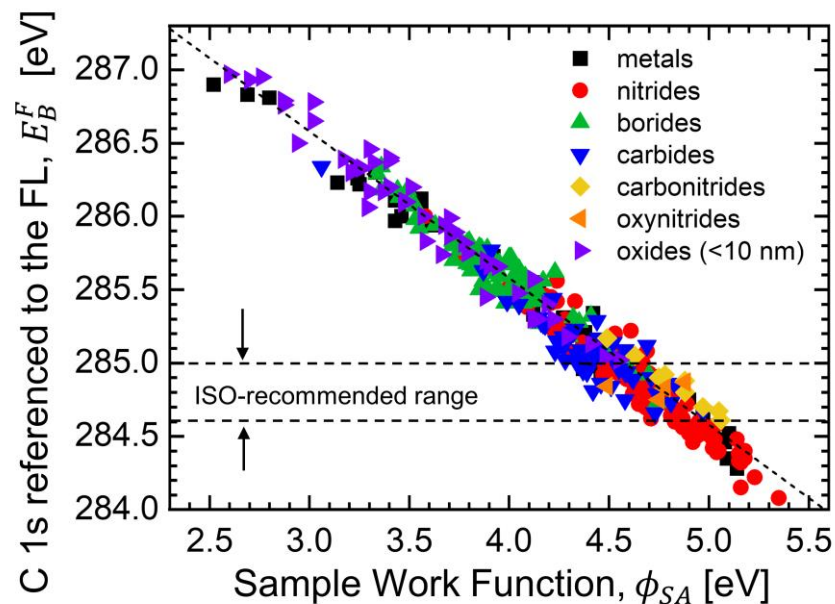


Figure 1 (color online) Binding energy of the C 1s peak corresponding to C-C/C-H bonds of adventitious carbon referenced to the Fermi level E_B^F plotted as a function of sample work function ϕ_{SA} assessed by UPS. 360 thin-film specimens spanning a wide range of material systems such as metals, nitrides, carbides, borides, oxides, carbonitrides, and oxynitrides are included. All samples are in the form of thin films and have been exposed to the ambient conditions for a time period ranging between several weeks and a few years.

In Fig. 1 the position of the C 1s C-C/C-H peak of AdC measured with respect to the spectrometers' FL E_B^F is plotted as a function of the sample work function ϕ_{SA} for more than

360 samples of metals, nitrides, borides, carbides, carbonitrides, oxynitrides, and oxides. The very close correlation between E_B^F and ϕ_{SA} is evident. In fact, the sum $E_B^F + \phi_{SA}$ is equal to 289.58 ± 0.12 eV. The average value agrees perfectly with previous results obtained for a limited sample set,¹⁹ while the standard deviation is reduced from 0.14 to 0.12 eV. The variation in the C 1s peak position is 2.89 eV, which is seven times more than the range specified in ISO guidelines, and more than many chemical shifts. Among samples showing the highest E_B^F of the C 1s peak are several metals such as Mg (286.90 eV, $\phi_{SA} = 2.52$ eV), Mg-Al alloy (286.83 eV, $\phi_{SA} = 2.69$ eV), and Y (286.81 eV, $\phi_{SA} = 2.8$ eV). Samples with lowest BE of the C 1s peak are several nitrides: MoN (284.08 eV, $\phi_{SA} = 5.35$ eV), WN (284.22 eV, $\phi_{SA} = 5.23$ eV), and VN (284.15 eV, $\phi_{SA} = 5.16$ eV). Such large C 1s shifts can be one possible reason for the large spread of BE values reported for the same chemical state in XPS data bases, e.g., 2.5 eV for the Zr 3d_{5/2} peak of ZrO₂, 2.3 eV for the Al 2p peak of Al₂O₃, 1.6 eV for the Na 1s peak of NaCl, 1.5 and 1.1 eV for the Si 2p peak from Si₃N₄ and SiO₂.²⁶

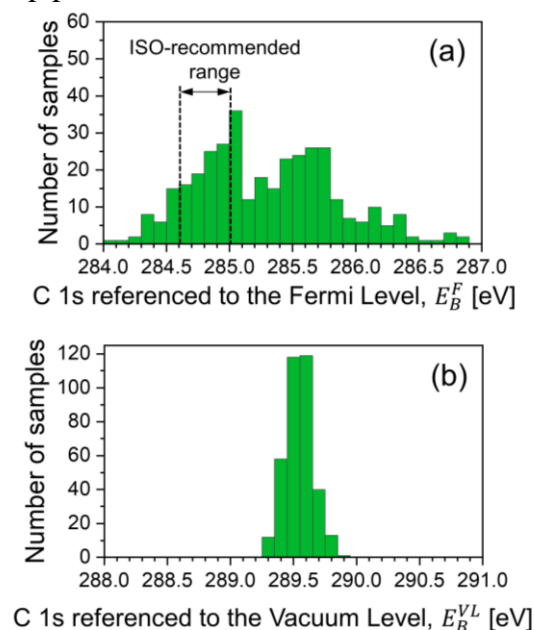


Figure 2 (color online) Histograms showing the distribution of the C 1s peak position referenced to (a) the Fermi level E_B^F , and (b) the Vacuum level E_B^{VL} . Plots illustrate differences between the conventional FL referencing and the VL referencing that involves the measurement of the sample work function. 360 thin-film specimens spanning a wide range of material systems such as metals, nitrides, carbides, borides, oxides, carbonitrides, and oxynitrides are included.

The subset of ultrathin oxide films is also added to Fig. 1. Such thin layers, insulating by nature, were recently shown to align to the VL provided that the oxide thickness is comparable to the electron penetration range such that the severe charging effects are prevented by the substrate electrons.²⁷ Up to the thickness of 12 nm the core level peaks from oxide (e.g. Al 2p from Al₂O₃) followed changes in the sample work function in the same manner as the C 1s peak of AdC. Hence, the VL alignment appears to be a general condition for thin layers with insulating properties (such as AdC and alumina) deposited on conducting substrates, fully confirming assessments made back in the early days of XPS.^{20,21,22}

Histograms presented in Fig. 2 show the distribution of (a) E_B^F , and (b) E_B^{VL} values for the C 1s peak of AdC, thus reflecting differences between the conventional FL referencing and the VL referencing that involves the measurement of the sample work function. In the latter case, the standard deviation is only 0.11 eV, i.e., less than the experimental resolution (~0.3 eV determined mostly by the X-ray width).

It has been suggested that the AdC C 1s peak shifts of the type illustrated in Fig. 1 are caused by the differential charging in the oxide layers that grown on the surface following longer storage in air.²⁸ Several experimental facts disprove this hypothesis. First, C 1s shifts by 2.5 eV also for samples stored for 14 h in UHV after oxides were removed by Ar etching.^{29,30} Secondly, C 1s shifts to higher BE are expected if the differential charging in the oxide should be the reason. However, for many samples the C 1s peaks are at lower binding energy than the “expected” 284.6-285.0 eV (see Fig. 1): for AdC on MoN, VN or WN (all with native oxides) the C 1s peak is found at 284.08, 284.15, and 284.22 eV, respectively. Such low E_B^F values, which directly disprove the differential charging hypothesis, are nicely explained within the framework of the VL alignment by very high work functions of these samples: 5.35, 5.16, and 5.23 eV. Furthermore, in the control experiment specifically designed to verify the “differential charging” hypothesis the C 1s from AdC on Al foil was consistently found at 286.4 eV,

irrespective of the native oxide thickness.³¹ The latter ranged from 0.7 to 4.7 nm, while the inelastic mean free path for Al 2p electrons in Al was 2.8 nm, i.e., 4 times longer than the minimum Al oxide thickness. It is unbelievable that such thin oxide could develop the positive potential of 1.6 V necessary to move the C 1s peak from the “standard” position of 284.8 eV. Finally, the E_B^F of the C 1s peak shows excellent correlation to the sample work function (cf. Fig. 1), which can not be explained by differential charging.

The VL alignment at the AdC/sample interface contradicts the implicit assumption behind the C 1s method, i.e., that the C 1s peak would appear at the constant BE, which is equivalent of claiming the FL alignment at the AdC/sample interface. The latter would, however, require significant charge transfer across the AdC/sample interface,^{25,32} which is contradicted by all experimental evidence about the AdC properties and behavior. The direct implication of the VL alignment is that the core levels from AdC shift as the sample work function changes.^{20,21,22,33} Hence, no meaningful referencing to the C 1s peak of AdC is possible without the simultaneous measurement of ϕ_{SA} . This is true irrespective of the experimental setup used: with samples grounded or isolated from spectrometer (with flood gun controlling the surface potential).

In fact, the VL alignment at the AdC/sample interface should not come as a surprise as AdC layers are not an inherent part of the analyzed sample. They are believed to be composed of aliphatic hydrocarbons and carboxide fragments,^{34,35} which typically do not form strong bonds to the surface and are easily removed in UHV by gentle heating.³⁶ Thus, they belong to the same category as weakly interacting thin films of saturated hydrocarbons prepared by spin-coating methods, for which VL alignment is well-proven.^{37,38,39,40} Such contacts often remain within the Schottky-Mott limit, where the electronic levels of the adsorbate are determined by the work function of the substrate.⁴¹ VL alignment for insulators have also been confirmed for model catalysts system consisting of Ni, Pd, and Pt on single crystal of α -alumina,⁴² adsorbates

on metal surfaces with sub-monolayer or monolayer coverage,^{43,44} and more recently for alumina films on conducting substrates.²⁷

The specific value of 289.58 ± 0.12 eV found for the C 1s peak of AdC referenced to VL compares well to values reported for the saturated hydrocarbon molecules. For example, Pireaux et al. reported 290.76 eV for C 1s from alkanes,⁴⁵ Karlsen et al. showed that the C 1s peak position varies from 290.71 eV for methane to 290.22 for octane.⁴⁶ Somewhat lower values were published for aromatic C moieties such as benzene (290.2 eV),⁴⁷ aniline (289.70 eV),⁴⁸ or phenol (290.2 eV).⁴⁸ All these values are 0.6 to 1.2 eV higher than the 289.58 ± 0.12 eV found for AdC. The latter value is, however, affected by the solid dielectric polarization energy and inter-molecular relaxation. The sum of both contributions, that are absent in the gas phase, can lower the measured BE by up to 1.5 eV.⁴⁹

In summary, the previous finding of the VL alignment at the AdC/sample interface is fully confirmed for a broader sample set comprising 360 thin-film specimens spanning a wide range of material systems such as metals, nitrides, carbides, borides, oxides, carbonitrides, and oxynitrides. The very close correlation between the C 1s position E_B^F and the sample work function ϕ_{SA} is confirmed to a better degree than in the previous paper. The variation in the C 1s peak position is 2.89 eV, which is seven times more than the range specified in ISO guidelines, and more than many chemical shifts. Several experimental observations disprove the hypothesis that the C 1s shifts are caused by differential charging. The direct implication of the VL alignment is that no meaningful referencing to the C 1s peak of AdC is possible without the simultaneous measurement of ϕ_{SA} . This conclusion applies irrespective of whether analyzes are conducted with samples grounded or intentionally isolated from the spectrometer (with flood gun controlling the surface potential).

The author most gratefully acknowledges the following researchers for making samples available: Babak Bakhit, Erik Lewin, Arnaud Le Febvrier, Ching-Lien Hsiao, Barbara Osinger,

Vladyslav Rogoz, Bartosz Wicher, Xiao Li, and Witold Gulbinski. The financial support from the Swedish Energy Agency under projects 51201-1 and P2023-00784, the Åforsk Foundation Grant 22-4, the Olle Engkvist Foundation grant 222-0053, the Swedish Government Strategic Research Area in Materials Science on Advanced Functional Materials at Linköping University (Faculty Grant SFO-Mat-LiU No. 2009-00971), and the Competence Center *Functional Nanoscale Materials* (FunMat-II) VINNOVA grant 2022-03071 is acknowledged.

Supplementary material

List of all samples included in the study along with measured binding energy values of the C-C/C-H component of the C 1s spectra of adventitious carbon referenced to the Fermi level E_B^F and to the vacuum level E_B^V , as well as the sample work function ϕ_{SA} assessed by UPS.

References

-
- ¹ ISO 15472:2010, "Surface chemical analysis -- X-ray photoelectron spectrometers -- Calibration of energy scales", (ISO, Geneva, 2010)
- ² J. Wolstenholme, "Procedure which allows the performance and calibration of an XPS instrument to be checked rapidly and frequently." *J. Vac. Sci. Technol. A* 38, 043206 (2020).
- ³ Seah MP. Summary of ISO/TC 201 Standard: VII ISO 15472: 2001—surface chemical analysis—x-ray photoelectron spectrometers—calibration of energy scales. *Surface and Interface Analysis*. 2001;31:721-3.
- ⁴ Siegbahn K, Nordling C. ESCA, atomic, molecular and solid state structure studied by means of electron spectroscopy. *Nov. Act. Uppsaliensis*. 1967
- ⁵ ISO 19318:2021 "Surface chemical analysis - Reporting of methods used for charge control and charge correction"
- ⁶ ASTM E1523-15, Standard Guide to Charge Control and Charge Referencing Techniques in X-Ray Photoelectron Spectroscopy, ASTM International, West Conshohocken, PA, 2015, www.astm.org
- ⁷ Hnatowich DJ, Hudis J, Perlman ML, Ragaini RC. Determination of charging effect in photoelectron spectroscopy of nonconducting solids. *Journal of Applied Physics*. 1971;42:4883-6.
- ⁸ Nordberg R, Brecht H, Albridge RG, Fahlman A, Van Wazer JR. Binding energy of the "2p" electrons of silicon in various compounds. *Inorganic Chemistry*. 1970;9:2469-74.
- ⁹ Kinoshita S, Ohta T, Kuroda H. Comments on the Energy Calibration in X-Ray Photoelectron Spectroscopy. *Bulletin of the Chemical Society of Japan*. 1976;49:1149-50.
- ¹⁰ Dianis WP, Lester JE. External standards in x-ray photoelectron spectroscopy. Comparison of gold, carbon, and molybdenum trioxide. *Analytical Chemistry*. 1973;45:1416-20.
- ¹¹ Johansson GG, Johansson J, Hedman A, Berndtsson M, Klasson R, Nilsson. *Journal of Electron Spectroscopy and Related Phenomena* 1973;2:295.
- ¹² Kohiki S, Oki K. Problems of adventitious carbon as an energy reference. *Journal of electron spectroscopy and related phenomena*. 1984;33:375-80.
- ¹³ Swift P. Adventitious carbon—the panacea for energy referencing? *Surface and Interface Analysis*. 1982;4:47-51.
- ¹⁴ Jacquemin M, Genet MJ, Gaigneaux EM, Debecker DP. Calibration of the X-Ray Photoelectron Spectroscopy Binding Energy Scale for the Characterization of Heterogeneous Catalysts: Is Everything Really under Control? *ChemPhysChem*. 2013;14:3618-26.
- ¹⁵ Yamashita T, Hayes P. Analysis of XPS spectra of Fe²⁺ and Fe³⁺ ions in oxide materials. *Applied Surface Science*. 2008;254:2441-9.
- ¹⁶ G. Greczynski and L. Hultman, „C 1s peak of adventitious carbon aligns to the vacuum level: dire consequences for material’s bonding assignment by photoelectron spectroscopy“, *ChemPhysChem* 18 (2017) 1507
- ¹⁷ G. Greczynski and L. Hultman, "X-ray photoelectron spectroscopy: towards reliable binding energy referencing", *Prog. Mat. Sci.* 107 (2020) 100591
- ¹⁸ G. Greczynski and L. Hultman, "The same chemical state of carbon gives rise to two peaks in x-ray photoelectron spectroscopy", *Scientific Reports* 11 (2021) 11195
- ¹⁹ G. Greczynski, Hultman L. Reliable determination of chemical state in x-ray photoelectron spectroscopy based on sample-work-function referencing to adventitious carbon: Resolving the myth of apparent constant binding energy of the C 1s peak. *Applied Surface Science*. 2018;451:99-103.
- ²⁰ P. Ascarelli, G. Missoni, Secondary electron emission and the detection of the vacuum level in ESCA. *Journal of Electron Spectroscopy and Related Phenomena* 5, 417-435 (1974).
- ²¹ R.T. Lewis, M.A. Kelly, Binding-energy reference in X-ray photoelectron spectroscopy of insulators. *Journal of Electron Spectroscopy and Related Phenomena* 20, 105-115 (1980).
- ²² Edgell, M. J., D. R. Baer, and J. E. Castle. "Biased referencing experiments for the XPS analysis of non-conducting materials." *Applied Surface Science* 26, no. 2 (1986): 129-149.
- ²³ G. Greczynski, S. Mráz, L. Hultman, J.M. Schneider, *Appl. Phys. Lett.* 2016, 108, 041603
- ²⁴ see for example: Chapter 1 in S. Hüfner "Photoelectron Spectroscopy: Principles and Applications", 3rd Ed. Springer 2003, ISSN 1439-2674
- ²⁵ H. Ishii, E. Sugiyama, E. Ito, and K. Seki, "Energy level alignment and interfacial electronic structures at organic/metal and organic/organic interfaces." *Advanced materials* 11 (1999): 605-625.

-
- ²⁶ NIST X-ray Photoelectron Spectroscopy Database, NIST Standard Reference Database Number 20, National Institute of Standards and Technology, Gaithersburg MD, 20899 (2000), DOI: <https://dx.doi.org/10.18434/T4T88K>, Accessed: 2024-04-23
- ²⁷ G. Greczynski, O.V. Pshyk, L. Hultman, "Towards an increased reliability of chemical bonding assignment in insulating samples by x-ray photoelectron spectroscopy", *Science Advances* 9 (2023) eadi3192
- ²⁸ Biesinger, Mark C. "Assessing the robustness of adventitious carbon for charge referencing (correction) purposes in XPS analysis: Insights from a multi-user facility data review." *Applied Surface Science* 597 (2022): 153681.
- ²⁹ Crist BV. "Handbooks of Monochromatic XPS Spectra – The Elements and Native Oxides, Volume 1". XPS Inter-national LLC: Mountain View, CA, USA, 1999.
- ³⁰ Crist, B. Vincent. "XPS in industry—Problems with binding energies in journals and binding energy databases." *Journal of Electron Spectroscopy and Related Phenomena* 231 (2019): 75-87.
- ³¹ G. Greczynski and L. Hultman, "Referencing to adventitious carbon in X-ray photoelectron spectroscopy: -can differential charging explain C 1s peak shifts?", *Appl. Surf. Sci.* 606 (2022) 154855
- ³² Lee, S. T., X. Y. Hou, Monica Gary Mason, and Ching Wan Tang. "Energy level alignment at Alq/metal interfaces." *Applied physics letters* 72 (1998): 1593-1595.
- ³³ H.D. Hagstrum, *Surf. Sci.* 1976, 54, 197
- ³⁴ Grey, Lauren H., Heng-Yong Nie, and Mark C. Biesinger. "Defining the nature of adventitious carbon and improving its merit as a charge correction reference for XPS." *Applied Surface Science* 653 (2024): 159319.
- ³⁵ Barr, Tery L., and Sudipta Seal. "Nature of the use of adventitious carbon as a binding energy standard." *Journal of Vacuum Science & Technology A: Vacuum, Surfaces, and Films* 13 (1995): 1239-1246.
- ³⁶ G. Greczynski and L. Hultman, *Appl. Phys. Lett.* 2016, 109, 211602
- ³⁷ Braun, Slawomir, William R. Salaneck, and Mats Fahlman. "Energy-level alignment at organic/metal and organic/organic interfaces." *Advanced materials* 21, no. 14-15 (2009): 1450-1472.
- ³⁸ Zhao, Jin, Min Feng, Daniel Barker Dougherty, Hao Sun, and Hrvoje Petek. "Molecular electronic level alignment at weakly coupled organic film/metal interfaces." *ACS nano* 8, no. 10 (2014): 10988-10997.
- ³⁹ Witte, Gregor, Simon Lukas, Paul S. Bagus, and Christof Wöll. "Vacuum level alignment at organic/metal junctions: "Cushion" effect and the interface dipole." *Applied Physics Letters* 87, no. 26 (2005).
- ⁴⁰ Willenbockel, M., D. Lüftner, B. Stadtmüller, G. Koller, C. Kumpf, S. Soubatch, P. Puschnig, M. G. Ramsey, and F. S. Tautz. "The interplay between interface structure, energy level alignment and chemical bonding strength at organic–metal interfaces." *Physical Chemistry Chemical Physics* 17, no. 3 (2015): 1530-1548.
- ⁴¹ E. H. Rhoderick and R.H. Williams, "Metal-Semiconductor contacts", Clarendon Press, Oxford, 1988
- ⁴² P. Legare, A. Fritsch, XPS study of transition metal/alumina model catalysts: Equilibrium and energy referencing. *Surface and Interface Analysis* 15, 698-700 (1990).
- ⁴³ K. Wandelt, J. E. Hulse, Xenon adsorption on palladium. I. The homogeneous (110),(100), and (111) surfaces. *The Journal of Chemical Physics* 80, 1340-1352 (1984).
- ⁴⁴ E. R. Kötz, H. Neff, K. Müller, A UPS, XPS and work function study of emersed silver, platinum and gold electrodes. *Journal of Electroanalytical Chemistry and Interfacial Electrochemistry* 215, 331-344 (1986).
- ⁴⁵ Pireaux, Jean-Jacques, S. Svensson, E. Basilier, P-Å. Malmqvist, U. Gelius, Roland Caudano, and K. Siegbahn. "Core-electron relaxation energies and valence-band formation of linear alkanes studied in the gas phase by means of electron spectroscopy." *Physical Review A* 14 (1976): 2133.
- ⁴⁶ Karlsen, Tor, Knut J. Børve, Leif J. Sæthre, Karoline Wiesner, Margit Bässler, and Svante Svensson. "Toward the spectrum of free polyethylene: Linear alkanes studied by carbon 1s photoelectron spectroscopy and theory." *Journal of the American Chemical Society* 124, (2002): 7866-7873.
- ⁴⁷ Myrseth, V., K. J. Børve, K. Wiesner, M. Bässler, S. Svensson, and L. J. Sæthre. "Vibrational structure and vibronic coupling in the carbon 1s photoelectron spectra of benzene and deuterobenzene." *Physical Chemistry Chemical Physics* 4, (2002): 5937-5943.
- ⁴⁸ Ohta, Toshiaki, Takashi Fujikawa, and Haruo Kuroda. "Core-electron spectra of mono-substituted benzenes obtained by the gas-phase X-ray photoelectron spectroscopy." *Bulletin of the Chemical Society of Japan* 48, (1975): 2017-2024.
- ⁴⁹ Pireaux, Jean-Jacques, and Roland Caudano. "X-ray photoemission study of core-electron relaxation energies and valence-band formation of the linear alkanes. II. Solid-phase measurements." *Physical Review B* 15, (1977): 2242.

Supplementary file

Binding energy referencing in X-ray photoelectron spectroscopy: expanded data set confirms that adventitious carbon aligns to the vacuum level

Grzegorz Greczynski

*Thin Film Physics Division, Department of Physics (IFM), Linköping University,
SE-581 83 Linköping, Sweden*

List of samples used in the analyses of C 1s peak position from adventitious carbon (AdC) and the work function measurement by UPS. If not otherwise indicated samples are in the form of thin films deposited by magnetron sputtering on Si(001) substrates. AdC is predominantly from air exposure except for a few cases where samples were first etched and then left overnight in the UHV chamber (as marked below).

	Sample	E_B^F [eV]	ϕ_{SA} [eV]	E_B^V [eV]	comments
1	Al	286.11	3.43	289.54	
2	Si	285.51	4.01	289.52	
3	Ti	285.29	4.15	289.44	
4	V	284.52	5.10	289.62	
5	Cr	284.59	4.79	289.38	
6	Y	286.41	3.26	289.67	
7	Zr	286.12	3.56	289.68	
8	Nb	285.37	4.37	289.74	
9	Hf	285.31	4.29	289.60	
10	Ta	285.73	3.98	289.71	
11	W	285.18	4.56	289.74	
12	Au	284.37	5.17	289.54	Foil
13	Ag	284.82	4.89	289.71	Foil
14	Sc	285.97	3.43	289.40	substrate: Al ₂ O ₃ (111)
15	Mn	285.21	4.31	289.52	
16	Mo	284.84	4.70	289.54	substrate: Al ₂ O ₃ (111)
17	Ni	285.19	4.18	289.37	
18	Cu	285.21	4.23	289.44	foil
19	Mg	286.00	3.46	289.46	Venting temperature T_v =400 °C
20	Al	286.23	3.14	289.37	foil
21	Fe	285.67	3.82	289.49	Foil
22	Mg	286.22	3.25	289.47	T_v =29 °C

23	Mg	286.90	2.52	289.42	Ar ⁺ -etched and exposed to UHV for 14 hours
24	Pt	284.54	4.96	289.5	
25	Co	284.96	4.37	289.33	
26	Cu18Mo82	284.66	4.85	289.51	
27	Cu30Mo70	285	4.6	289.6	
28	Cu35Mo65	284.95	4.46	289.41	
29	Cu41Mo59	285.03	4.57	289.6	
30	Cu46Mo54	285.09	4.41	289.5	
31	Cu58Mo42	284.99	4.48	289.47	
32	Cu68Mo32	285.26	4.34	289.6	
33	Cu73Mo27	285.21	4.38	289.59	
34	Cu77Mo23	285.06	4.45	289.51	
35	Cu82Mo18	285.04	4.47	289.51	
36	Cu88Mo12	285.06	4.45	289.51	
37	Ti8V28Mo53Nb5W26	284.75	4.9	289.65	
38	Ti6V33Mo24Nb7W30	284.65	4.97	289.62	
39	Ti6V23Mo9Nb24W38	284.46	5.08	289.54	
40	Ti4V18Mo23Nb6W49	284.35	5.09	289.44	
41	Ti3V23Mo9Nb24W38	284.82	4.85	289.67	
42	Fe65Ti13Co8Ni7Nb1	284.92	4.57	289.49	
43	MgAl	286.83	2.69	289.52	AZ31 soild
44	Co23Cr15Ni16Fe46	285.25	4.26	289.51	
45	Co22Cr15Ni16Fe47	285.34	4.42	289.76	
46	Co23Cr19Ni14Fe44	285.51	4.15	289.66	
47	Co24Cr18Ni13Fe45	285.55	4.12	289.67	
48	Co24Cr28Ni10Fe38	285.43	4.17	289.6	
49	Co24Cr25Ni10Fe41	285.34	4.42	289.76	
50	TiN	284.52	4.9	289.42	
51	VN	284.15	5.16	289.31	
52	CrN	284.6	4.83	289.43	
53	ZrN	285.49	4.09	289.58	
54	NbN	284.98	4.48	289.46	
55	MoN	284.08	5.35	289.43	
56	HfN	285.52	4	289.52	
57	TaN	285.08	4.41	289.49	
58	WN	284.22	5.23	289.45	
59	TiN	284.68	4.70	289.38	$T_v = 29\text{ }^\circ\text{C}$
60	TiN	284.65	4.69	289.34	$T_v = 330\text{ }^\circ\text{C}$
61	TiN	284.62	4.71	289.33	steel substrate
62	Ti _{0.84} Ta _{0.16} N	284.70	4.68	289.38	
63	Ti _{0.62} Ta _{0.38} N	284.72	4.65	289.37	
64	Ti _{0.39} Ta _{0.61} N	284.92	4.47	289.39	
65	Ti _{0.21} Ta _{0.79} N	285.09	4.29	289.38	
66	Ti _{0.14} Ta _{0.86} N	285.21	4.26	289.47	
67	Ti _{0.07} Ta _{0.93} N	285.23	4.22	289.45	

68	Zr _{0.93} Al _{0.07} N	285.46	4.18	289.64	
69	Zr _{0.66} Al _{0.34} N	285.74	4.08	289.82	
70	Zr _{0.75} Al _{0.25} N	285.59	4.20	289.79	
71	Zr _{0.37} Al _{0.63} N	285.82	3.79	289.61	
72	ZrN	285.45	4.21	289.66	steel substrate
73	Zr _{0.73} Al _{0.27} N	285.42	4.24	289.66	
74	Zr _{0.84} Al _{0.16} N	285.41	4.21	289.62	
75	Cr _{0.82} Al _{0.18} N	284.77	4.70	289.47	
76	Cr _{0.71} Al _{0.29} N	284.75	4.72	289.47	
77	Cr _{0.61} Al _{0.39} N	284.83	4.63	289.46	
78	Cr _{0.54} Al _{0.46} N	284.92	4.56	289.48	
79	Cr _{0.45} Al _{0.55} N	284.99	4.51	289.50	
80	Cr _{0.34} Al _{0.66} N	285.04	4.45	289.49	
81	Cr _{0.23} Al _{0.77} N	285.04	4.45	289.49	
82	Cr _{0.15} Al _{0.85} N	285.14	4.37	289.51	
83	Ti _{0.84} Al _{0.16} N	284.91	4.64	289.55	
84	Ti _{0.75} Al _{0.25} N	284.80	4.82	289.62	
85	Ti _{0.65} Al _{0.35} N	284.93	4.70	289.63	
86	Ti _{0.50} Al _{0.50} N	285.08	4.69	289.77	
87	Ti _{0.46} Al _{0.54} N	285.20	4.53	289.73	
88	Ti _{0.41} Al _{0.59} N	285.04	4.65	289.69	
89	Ti _{0.34} Al _{0.66} N	285.22	4.61	289.83	
90	Ti _{0.24} Al _{0.76} N	285.41	4.46	289.87	
91	Ti92W8N	284.9	4.59	289.49	
92	Ti85Al7W8N	284.91	4.56	289.47	
93	Ti68Al24W8N	285.08	4.51	289.59	
94	Ti62Al30W8N	284.79	4.62	289.41	
95	Ti52Al40W8N	285	4.52	289.52	
96	Ti43Al49W8N	284.89	4.59	289.48	
97	Ti36Al56W8N	284.92	4.49	289.41	
98	Ti28Al64W8N	285.06	4.4	289.46	
99	Ti6V22Mo37Nb5W30N	284.4	5.05	289.45	
100	V17Mo43W40N	284.35	5.18	289.53	
101	Ti4V17Mo27Nb5W47N	284.4	5.18	289.58	
102	V14Mo27W59N	284.38	5.15	289.53	
103	V11Mo20W69N	284.33	5.15	289.48	
104	V4Mo17W79N	284.6	4.95	289.55	
105	V22Mo29W49N	284.58	5.04	289.62	
106	V31Mo27W42N	284.32	5.16	289.48	
107	Ti8V28Mo28Nb8W27N	284.48	5.14	289.62	
108	Hf89Si11N	285.3	4.28	289.58	
109	Hf86Si14N	285.42	4.33	289.75	
110	Hf82Si18N	285.56	4.24	289.8	
111	Hf68Si32N	286	3.58	289.58	
112	Ti0.89Si0.11N	284.85	4.7	289.55	
113	Ti0.77Si0.23N	284.88	4.77	289.65	

114	Ti _{0.62} Si _{0.38} N	284.72	4.8	289.52	
115	Ti _{0.54} Si _{0.46} N	284.87	4.71	289.58	
116	Ti _{0.47} Si _{0.53} N	284.95	4.65	289.6	
117	Ti _{0.36} Si _{0.64} N	285	4.67	289.67	
118	Ti _{0.23} Si _{0.77} N	284.93	4.62	289.55	
119	Ti _{0.11} Si _{0.89} N	285.04	4.45	289.49	
120	Mo ₇₂ V ₂₇ N	284.56	4.99	289.55	
121	Mo ₆₀ V ₄₀ N	284.53	4.97	289.5	
122	Mo ₆₅ V ₃₅ N	284.48	5.03	289.51	
123	Mo ₅₀ V ₅₀ N	284.39	5.04	289.43	
124	Mo ₅₂ V ₄₈ N	284.46	4.92	289.38	
125	Mo ₆₂ V ₃₈ N	284.52	4.96	289.48	
126	Mo ₅₁ V ₄₉ N	284.54	5	289.54	
127	Mo ₅₀ V ₅₀ N	284.42	5.02	289.44	
128	Mo ₄₇ V ₅₃ N	284.52	4.98	289.5	
129	Mo ₄₅ V ₅₅ N	284.48	5.02	289.5	
130	V ₈₄ Al ₁₆ N	284.68	4.82	289.5	
131	V ₇₇ Al ₂₃ N	284.78	4.67	289.45	
132	V ₆₇ Al ₃₃ N	284.82	4.68	289.5	
133	V ₆₁ Al ₃₉ N	284.76	4.67	289.43	
134	V ₅₅ Al ₄₅ N	284.81	4.64	289.45	
135	V ₅₀ Al ₅₀ N	285.04	4.56	289.6	
136	V ₄₅ Al ₅₅ N	285	4.5	289.5	
137	V ₄₀ Al ₆₀ N	284.95	4.62	289.57	
138	V ₃₄ Al ₆₆ N	284.95	4.62	289.57	
139	V ₃₀ Al ₇₀ N	284.96	4.63	289.59	
140	V ₂₆ Al ₇₄ N	284.85	4.72	289.57	
141	V ₂₀ Al ₈₀ N	284.78	4.71	289.49	
142	V ₁₆ Al ₈₄ N	284.74	4.75	289.49	
143	Cr ₉₉ N ₁	284.77	4.76	289.53	
144	Cr ₉₅ N ₅	284.72	4.89	289.61	
145	Cr ₈₉ N ₁₁	284.68	4.84	289.52	
146	Cr ₈₅ N ₁₅	284.63	4.86	289.49	
147	Cr ₇₈ N ₂₂	284.6	4.86	289.46	
148	Cr ₇₅ N ₂₅	284.56	4.87	289.43	
149	Cr ₇₃ N ₂₇	284.62	4.87	289.49	
150	Cr ₆₄ N ₃₆	284.54	4.92	289.46	
151	Cr ₅₈ N ₄₂	284.54	4.91	289.45	
152	Cr ₅₆ N ₄₄	284.64	4.81	289.45	
153	Cr ₅₃ N ₄₇	284.5	4.94	289.44	
154	Cr ₄₆ N ₅₄	284.56	4.91	289.47	
155	TiB ₂	285.40	4.47	289.97	
156	ZrB ₂	285.59	4.30	289.89	
157	Al _{0.10} Mg _{0.07} B _{0.83}	286.29	3.34	289.63	
158	Al _{0.07} Mg _{0.08} B _{0.85}	286.18	3.49	289.67	
159	Al _{0.09} Mg _{0.13} B _{0.78}	286.18	3.44	289.62	

160	Al _{0.08} Mg _{0.08} B _{0.84}	286.07	3.53	289.60	
161	Al _{0.07} Mg _{0.03} B _{0.90}	286.18	3.36	289.54	
162	Al _{0.07} Mg _{0.06} B _{0.87}	286.34	3.36	289.70	
163	Al _{0.08} Mg _{0.16} B _{0.76}	286.11	3.50	289.61	
164	Ti _{0.64} Al _{0.36} B _{1.93}	285.84	3.72	289.56	
165	Ti _{0.51} Al _{0.49} B _{1.97}	285.68	3.95	289.63	
166	Ti _{0.42} Al _{0.58} B _{1.87}	285.78	3.86	289.64	
167	Ti _{0.38} Al _{0.62} B _{1.92}	285.7	3.87	289.57	
168	Ti _{0.33} Al _{0.67} B _{1.83}	285.82	3.79	289.61	
169	Ti _{0.26} Al _{0.74} B _{1.82}	285.78	3.77	289.55	
170	Ti _{0.6} Al _{0.4} B _{2.03}	285.64	3.94	289.58	
171	Ti _{0.26} Al _{0.74} B _{1.86}	285.77	3.78	289.55	
172	Ti _{0.24} Al _{0.76} B _{1.81}	285.81	3.72	289.53	
173	AlB _{11.5}	285.09	4.5	289.59	
174	AlB _{3.27}	285.7	3.88	289.58	
175	AlB _{2.75}	285.66	3.91	289.57	
176	AlB _{2.5}	285.55	4.02	289.57	
177	AlB _{2.3}	285.53	4.09	289.62	
178	AlB _{2.2}	285.94	3.63	289.57	
179	AlB _{1.83}	285.5	4.1	289.60	
180	Ti ₈₅ Si ₁₅ B _{2.44}	285.59	4.08	289.67	
181	Ti ₇₅ Si ₂₅ B _{2.07}	285.67	4.02	289.69	
182	Ti ₆₉ Si ₃₁ B _{1.77}	285.69	4.02	289.71	
183	Ti ₈₆ Si ₁₄ B _{2.39}	285.62	4.23	289.85	
184	Ti ₇₇ Si ₂₃ B _{2.06}	285.56	4.17	289.73	
185	Ti ₇₂ Si ₂₈ B _{1.84}	285.51	4.13	289.64	
186	Ti ₆₂ Si ₃₈ B _{1.55}	285.64	4.16	289.8	
187	HfB ₂	285.79	3.85	289.64	
188	W ₂ B ₅	285.28	4.35	289.63	
189	TiWB _{2.1}	285.28	4.35	289.63	
190	TiWB _{2.3}	285.31	4.32	289.63	
191	VB ₂	284.73	4.74	289.47	
192	VB ₂	285.32	4.41	289.73	Ar ⁺ -etched and exposed to UHV for 14 hours
193	TaB ₂	285.5	4	289.5	
194	CrB _{1.9}	285.06	4.51	289.57	
195	CrB _{1.8}	284.96	4.6	289.56	
196	CrB _{1.75}	284.92	4.7	289.62	
197	Zr ₇₇ Cr ₂₃ B _{1.5}	285.5	3.85	289.35	
198	Zr ₇₁ Cr ₂₉ B _{1.42}	285.7	3.72	289.42	
199	Zr ₆₈ Cr ₃₂ B _{1.38}	285.53	3.84	289.37	
200	Zr ₆₄ Cr ₃₆ B _{1.3}	285.51	3.88	289.39	
201	Zr ₅₆ Cr ₄₄ B _{1.11}	285.68	3.79	289.47	
202	Zr ₇₁ Cr ₂₉ B _{1.42}	285.49	3.94	289.43	Ar ⁺ -etched and exposed to UHV for 14 hours

203	Zr68Cr32B1.38	285.56	3.87	289.43	Ar ⁺ -etched and exposed to UHV for 14 hours
204	Zr64Cr36B1.3	285.63	3.81	289.44	Ar ⁺ -etched and exposed to UHV for 14 hours
205	Zr56Cr44B1.11	285.67	3.81	289.48	Ar ⁺ -etched and exposed to UHV for 14 hours
206	Zr52V48B2	285.18	4.3	289.48	
207	Z46rV54B2	285.22	4.16	289.38	
208	Zr0.9Nb0.1B2	285.66	3.84	289.5	
209	Zr0.8Nb0.2B2	285.83	3.72	289.55	
210	Zr0.7Nb0.3B2	285.8	3.72	289.52	
211	Zr0.9Ta0.1B2.1	285.65	3.84	289.49	
212	Zr0.8Ta0.2B1.8	285.72	3.81	289.53	
213	Zr0.7Ta0.3B1.5	285.7	3.83	289.53	
214	ZrB2.3	285.7	3.79	289.49	
215	Ti15Al28B57	285.98	3.53	289.51	
216	Ti14Al29B57	285.48	4.15	289.63	
217	Ti12Al28B60	285.41	4.07	289.48	
218	Ti16Al30B54	285.77	3.77	289.54	
219	Ti27Al11B62	285.44	4.06	289.5	
220	Ti17Al27B57	285.71	3.83	289.54	
221	Ti18Al26B56	285.68	3.86	289.54	
222	Ti19Al23B58	285.67	3.89	289.56	
223	Ti17Al28B55	285.72	3.82	289.54	
224	Ti18Al24B58	285.71	3.87	289.58	
225	Ti19Al23B58	285.67	3.92	289.59	
226	Ti19Al24B57	285.69	3.88	289.57	
227	Ti15Al30B55	286.13	3.45	289.58	
228	Ti14Al36B50	285.78	3.78	289.56	
229	Ti27Al19B54	285.76	3.89	289.65	
230	Hf17Ti22B61	285.63	3.88	289.51	
231	Hf24Ti21B55	285.52	3.94	289.46	
232	Hf10Ti30B60	285.42	4.14	289.56	
233	Hf15Ti29B56	285.42	4.1	289.52	
234	Hf26Ti22B52	285.72	4	289.72	
235	Hf39Ti7B54	285.83	3.8	289.63	
236	Hf20Ti22B58	285.59	4.02	289.61	
237	Hf25Ti22B53	285.72	3.89	289.61	
238	Hf42Ti5B53	285.85	3.75	289.6	
239	TiBx	285.59	3.95	289.54	
240	Ti77Hf33B1.7	285.51	4.05	289.56	
241	TiHfB	285.53	4.06	289.59	
242	TiHfB	285.64	4.05	289.69	
243	TiBx	285.48	4.02	289.5	
244	Hf46B54	285.78	3.86	289.64	
245	Hf47B53	285.92	3.55	289.47	

246	HfB	285.61	3.94	289.55	
247	Hf51B49	285.61	3.94	289.55	
248	Hf49B51	285.67	3.9	289.57	
249	Hf52B48	285.69	3.93	289.62	
250	Hf55B45	285.78	3.89	289.67	
251	TiC	284.92	4.76	289.68	
252	VC	284.67	4.97	289.64	
253	CrC	284.86	4.83	289.69	
254	NbC	284.98	4.82	289.80	
255	MoC	284.83	4.93	289.76	
256	Ni74Cr22C4	285.31	4.13	289.44	
257	Ni73Cr21C6	285.23	4.33	289.56	
258	Ni69Cr20C11	285.18	4.27	289.45	
259	Ni57Cr22C21	285.08	4.23	289.31	
260	Ni52Cr21C27	285	4.34	289.34	
261	Ni36Cr16C48	285.11	4.27	289.38	
262	Ni26Cr11C63	285.02	4.28	289.3	
263	ZrC	285.14	4.48	289.62	
264	HfC	285.44	4.22	289.66	
265	TaC	285.14	4.52	289.66	
266	WC	285.09	4.58	289.67	
267	WC1.2	284.89	4.62	289.51	
268	WC1.5	285.29	4.44	289.73	
269	WC1.5	285.12	4.69	289.81	Ar ⁺ -etched and exposed to UHV for 14 hours
270	Ti41C59	284.84	4.51	289.35	
271	Ti43C57	284.75	4.58	289.33	
272	Ti47C53	285.03	4.56	289.59	
273	Ti54C46	285.06	4.34	289.4	
274	Ti51C49	285.04	4.52	289.56	
275	Ti45C55	284.96	4.55	289.51	
276	Ti42C58	284.94	4.59	289.53	
277	Ti41C59	284.94	4.58	289.52	
278	Ti55C45	284.79	4.74	289.53	
279	Ni68Mo22C10	285.26	4.18	289.44	
280	Ni69Mo21C10	285.05	4.43	289.48	
281	Ni70Mo20C10	285.04	4.43	289.47	
282	Ni62Mo22C16	285.08	4.42	289.5	
283	Ni57Mo19C24	285.09	4.36	289.45	
284	Ni43Mo14C43	284.94	4.39	289.33	
285	Ni28Mo9C63	284.81	4.42	289.23	
286	Ni19Mo5C76	284.86	4.46	289.32	
287	ZrTi2AlC	285.63	3.87	289.5	
288	V9Al28C63	285.28	4.17	289.45	
289	V10Al32C58	285.31	4.15	289.46	
290	V12Al33C55	285.28	4.16	289.44	

291	V11Al35C54	285.27	4.17	289.44	
292	V12Al34C54	285.31	4.13	289.44	
293	V10Al36C54	285.42	3.99	289.41	
294	HfC	286.34	3.06	289.4	
295	ZrC	285.4	4.05	289.45	
296	WC	285.06	4.39	289.45	
297	NbC	284.66	4.73	289.39	
298	VC	284.73	4.81	289.54	
299	NbC	285.77	3.91	289.68	
300	TaC	285.15	4.24	289.39	
301	MoC	284.95	4.37	289.32	
302	V _{0.18} Al _{0.31} O _{0.03} N _{0.48}	284.90	4.75	289.65	
303	V _{0.16} Al _{0.34} O _{0.03} N _{0.47}	284.92	4.78	289.70	
304	V _{0.16} Al _{0.34} O _{0.04} N _{0.46}	284.88	4.88	289.76	
305	V _{0.17} Al _{0.33} O _{0.07} N _{0.43}	285.17	4.49	289.66	
306	V _{0.19} Al _{0.33} O _{0.11} N _{0.38}	285.05	4.63	289.68	
307	V _{0.20} Al _{0.33} O _{0.17} N _{0.30}	284.80	4.88	289.68	
308	V _{0.22} Al _{0.30} O _{0.25} N _{0.23}	284.70	4.97	289.67	
309	V _{0.24} Al _{0.28} O _{0.30} N _{0.18}	284.67	5.05	289.72	
310	V _{0.19} Al _{0.35} O _{0.38} N _{0.08}	284.61	5.06	289.67	
311	Cr92C6N2	284.75	4.77	289.52	
312	Cr72C20N8	284.83	4.82	289.65	
313	Cr64C25N11	284.87	4.81	289.68	
314	Cr62C32N6	284.84	4.79	289.63	
315	Ta ₂ O ₅	286.10	3.48	289.58	
316	TiO ₂	285.30	4.22	289.52	
317	Al ₂ O ₃ (10nm)/Al	286.97	2.6	289.57	
318	Al ₂ O ₃ (10nm)/W	286.34	3.23	289.57	
319	Al ₂ O ₃ (10nm)/TiN	286.65	3.02	289.67	
320	Al ₂ O ₃ (10nm)/HfN	287.28	2.2	289.48	
321	Al ₂ O ₃ (10nm)/Si	286.76	2.87	289.63	
322	Al ₂ O ₃ (10nm)/VN	286.38	3.4	289.78	
323	Al ₂ O ₃ (10nm)/V	286.37	3.32	289.69	
324	Al ₂ O ₃ (10nm)/WN	286.33	3.26	289.59	
325	Al ₂ O ₃ (10nm)/Zr	286.93	2.7	289.63	
326	Al ₂ O ₃ (2nm)/Al	286.5	2.94	289.44	
327	Al ₂ O ₃ (2nm)/W	285.45	3.88	289.33	
328	Al ₂ O ₃ (2nm)/MoN	285.13	4.41	289.54	
329	Al ₂ O ₃ (2nm)/TiN	285.57	4.12	289.69	
330	Al ₂ O ₃ (2nm)/HfN	286.78	3.02	289.8	
331	Al ₂ O ₃ (2nm)/Si	286.17	3.37	289.54	
332	Al ₂ O ₃ (2nm)/VN	285.04	4.48	289.52	
333	Al ₂ O ₃ (2nm)/V	285.18	4.29	289.47	
334	Al ₂ O ₃ (2nm)/WN	285.66	3.9	289.56	
335	Al ₂ O ₃ (2nm)/Zr	286.3	3.21	289.51	
336	Al ₂ O ₃ (4.8nm)/Al	286.17	3.3	289.47	

337	Al2O3(5.8nm)/Al	286.39	3.17	289.56	
338	Al2O3(3.7nm)/Al	286.06	3.29	289.35	
339	Al2O3(7.3nm)/Al	286.79	2.87	289.66	
340	Al2O3(11.8nm)/Al	286.95	2.76	289.71	
341	Al2O3(1.1nm)/W	285.3	4.12	289.42	
342	Al2O3(4nm)/W	285.74	3.66	289.4	
343	Al2O3(6nm)/W	285.83	3.58	289.41	
344	Al2O3(8nm)/W	286.09	3.47	289.56	
345	Al2O3(12nm)/W	286.46	3.3	289.76	
346	SiO2(1nm)/W	285.4774	4.04	289.52	
347	SiO2(2nm)/W	285.659	3.94	289.6	
348	SiO2(4nm)/W	285.7508	3.79	289.54	
349	SiO2(6nm)/W	285.8166	3.77	289.59	
350	SiO2(8nm)/W	285.8671	3.70	289.57	
351	SiO2(10nm)/W	285.8933	3.73	289.62	
352	SiO2(12nm)/W	285.9381	3.67	289.61	
353	SiO2(15nm)/W	285.9889	3.70	289.69	
354	HfO2(1nm)/W	285.3	4.14	289.44	
355	HfO2(2nm)/W	285.4	4.19	289.59	
356	HfO2(4nm)/W	285.7	3.88	289.58	
357	HfO2(6nm)/W	286	3.57	289.57	
358	HfO2(8nm)/W	286.1	3.47	289.57	
359	HfO2(10nm)/W	286.2	3.4	289.6	
360	HfO2(12nm)/W	286.2	3.51	289.71	
361	HfO2(15nm)/W	286.4	3.4	289.8	
362	CuO(10nm)/W	285.02	4.55	289.57	